

NUMERICAL AND EXPERIMENTAL STUDY FOR THE CHARACTERIZATION OF THE SPALLATION TARGET PERFORMANCE OF THE ULTRACOLD NEUTRON SOURCE AT THE PAUL SCHERRER INSTITUT

V. Talanov* and M. Wohlmuther, Paul Scherrer Institut, Villigen, Switzerland,
on behalf of the UCN Project Team†

Abstract

Results of numerical calculations and the experimental characterization of the neutron flux profile at the ultracold neutron (UCN) source of the Paul Scherrer Institut (PSI) are presented. At first, the MCNPX-based model of the Monte-Carlo simulation with its detailed description of the so-called “Cannelloni”-type spallation target assembly and the realistic proton beam profile modeling is described. Thereafter the experimental determination of the thermal neutron flux profile using gold foil activation, along the height of the UCN tank, starting from the proton beam plane, is presented. Both calculations and measurements were performed for standard beam parameters, with the full proton beam on target. Finally, a comparison of simulation and experimental result is discussed.

INTRODUCTION

The ultracold neutron (UCN) source at PSI [1] operates in pulsed mode, with a pulse duration of up to 8 s and full proton current of up to 2.4 mA. The proton beam is delivered from the PSI high intensity accelerator complex [2] onto the “Cannelloni”-type spallation target [3] of the UCN source. To characterize the UCN target performance “as built”, an aluminum tube suitable for inserting miniature neutron detectors and gold foils was installed in the gap between the UCN tank and the innermost shielding, covering the full height of the tank. During UCN source operation in 2012 gold foils were inserted through this tube down to the beam plane. Their induced activity was then analyzed and is compared to the results of numerical simulations.

MODEL OF THE MCNPX SIMULATION

To characterize the target performance, neutron flux density distributions and neutron spectra around the UCN source were simulated using MCNPX 2.7.0 [4]. The detailed 3D model of the UCN source, used in the MCNPX simulation for the results in this paper, was inherited from [3], with only minor modifications for the insertion tube position and corresponding tallys.

The UCN Source

The side view of the central part of the UCN source is illustrated by the photo in Fig. 1 (left). The outer shell

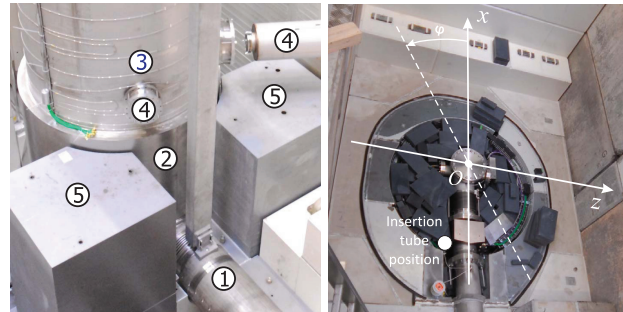


Figure 1: Left: side view of the UCN source, at the start of the inner shielding installation: only one block at each side of the target is present. Right: top shielding of the UCN source, with the coordinate system of the MCNPX model. All labels are explained in text.

of the target (1), through which the spallation target is inserted, continues as a vacuum chamber through the cylindrical D₂O moderator (2). At the top of the D₂O, inside the tank (3), the UCN storage volume is located, connected to the horizontal UCN guides (4). In the simulation model the UCN tank was fully enclosed first by the inner shielding iron blocks (5), and then by the biological shielding (not seen in the photo).

The coordinate system, used in the MCNPX simulation and in the presentation of the results later in this paper, is superimposed over the photo of the UCN top shielding in Fig. 1 (right, at $y = 503$ cm). The incoming beam at the target was directed along the z axis, the y axis was the vertical axis of the UCN source, and the xOz plane at $y = 0$ cm was the “beam” plane. The white spot in Fig. 1 (right) indicates the insertion tube position at $(z, x) = (-23, -93)$ cm.

Spallation Target

The model of the UCN source spallation target used in the MCNPX simulation is illustrated in Fig. 2. The model contained a representation of the “Cannelloni”-type target assembly [3], including a detailed description of the target array made of lead-filled Zircaloy tubes (1), as well as other essential details of the target — the target safety shroud (2), the forward neutron Pb shielding cylinder (3) and target container filled with the D₂O coolant (4). The target was positioned inside the vacuum chamber that intersected the D₂O moderator tank (5).

* vadim.talanov@psi.ch

† ucn.web.psi.ch

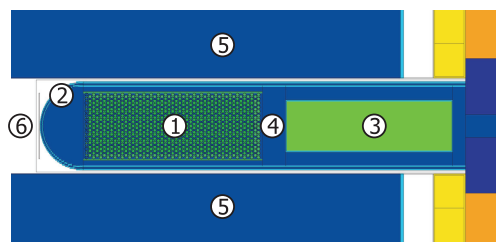


Figure 2: Vertical zy cut of the MCNPX “Cannelloni”–type spallation target model.

Proton Beam

The proton beam in the simulations was started in the geometry cell in front of the target, at $z = -31$ cm from the vertical y axis of the UCN source (6, Fig. 2). The incident proton beam energy was equal to 590 MeV. The shape and the intensity of the beam at the target was taken according to separate beam optics calculation [5]. The beam profile was assumed to follow a 2D Gaussian distribution with $\sigma_{x,y} = 4$ cm cut at $r = 10$ cm from the central beam axis. The results of the MCNPX simulation were normalized to 1 s pulse duration and a beam intensity 95 % of the nominal 2.2 mA value.

EXPERIMENTAL DETERMINATION OF THE NEUTRON FLUX PROFILE

The neutron flux profile along the height of the UCN tank was studied by the activation of gold foils. Gold foils of 25 mm diameter were used in the experimental procedure. The foils were pushed down into the insertion tube on a 7 mm diameter nylon rope. Each individual foil was wrapped around the rope with an 1 mm thick aluminum clamping. All these details were taken into account in the model of the MCNPX simulation of the neutron spectra at the exact location of the gold foil.

The mass of each foil was measured before the activation. After irradiation the activity of each foil was analyzed using γ -spectroscopy. The specific activity, a (Bq/g), of the ^{198}Au nuclide in each foil was derived and then re-scaled to the beam intensity assumed in the simulation.

SIMULATED NEUTRON FLUX DENSITY

The neutron flux density in the 4 cm gap between the inner shielding (1) and the D_2O tank (2) at the beam plane, as simulated by MCNPX is given in Fig. 3. The distribution has a clear maximum at $\phi = 90^\circ$ around the center of the incoming beam, due to backscattering from the target (3). At the opposite side of the spallation target ($\phi = 270^\circ$), the observed dip in the flux density corresponds to the position of the Pb shielding cylinder (4).

The insertion tube position at the beam plane ($\phi = 166^\circ$) falls into the region of slowly increasing neutron flux density. The uncertainty of the verticality for the neutron detector tube was estimated as $\pm 1.5^\circ$. With the length of 503

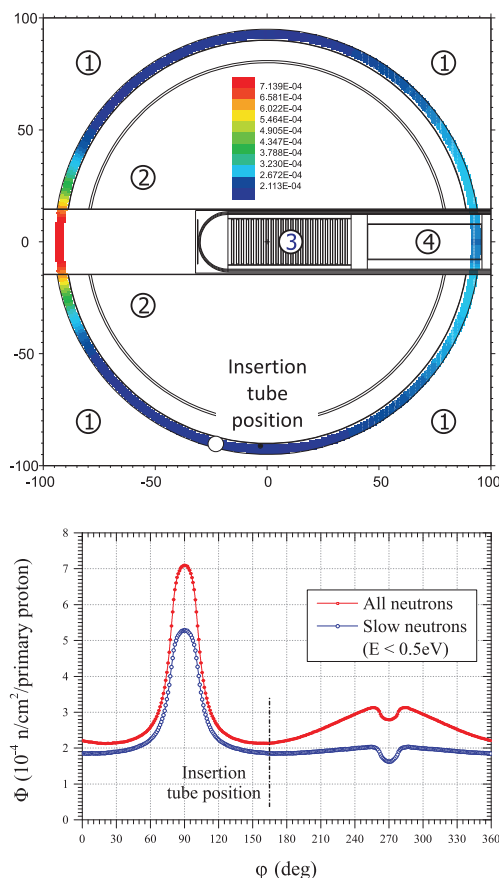


Figure 3: Neutron flux density, Φ ($\text{n}/\text{cm}^2/\text{proton}$), distribution at the beam plane around the D_2O tank, as a function of (z, x) coordinates (top) and azimuthal angle ϕ (bottom).

cm of the tube from the insertion position down to the beam plane, this gives an uncertainty of the tube position at the beam plane of ± 13.9 cm along the outer surface of the D_2O tank. To study the influence of this uncertainty on the measured gold foil activity, neutron spectra were tallied in the MCNPX simulation at four additional locations around the D_2O tank, at ± 10 and ± 20 cm from the ideal position of the insertion tube.

GOLD FOIL ACTIVITY CALCULATION

The estimates of the neutron flux density and the neutron spectra, obtained in the MCNPX simulation of the UCN source model, were used to calculate the nuclide inventory in the gold foil with the Activation Script [6]. The Activation Script has been developed by a collaboration of ORNL, ANL, LANL and PSI [7]. This tool provides to the user an automated procedure to extract the required data from the MCNPX output, to prepare the input files and to run different activation codes to calculate the list of nuclides and their activity according to given irradiation and cooling history. For the results in the present paper, the FISPACT code was used [8].

COMPARISON OF THE NUMERICAL RESULTS TO THE MEASUREMENT

In addition to the uncertainty of the insertion tube position at the beam plane, the comparison between results of the simulation and measurements shall account for the uncertainty of the gold foils vertical position in the tube (y axis of the MCNPX geometry model). For this, the neutron spectra for the activity calculation were tallied in the simulation along the y axis in a region of ± 20 cm around the beam plane, in 1 cm steps.

Yet another uncertainty comes from the composition of the UCN source inner shielding (1, Fig. 3) which is close to the one of the cast iron (standard shielding material 162 [9]). To evaluate it, three cases were simulated, using as material for the shielding: a) standard air (no shielding), b) cast iron, $\rho = 7.15 \text{ g/cm}^3$ and c) pure iron, $\rho = 7.87 \text{ g/cm}^3$. Neutron spectra for these three cases are given in Fig. 4. The $\sim 10\%$ spread in the spectra estimates for the energy range of $0.5 \text{ eV} \div 10 \text{ keV}$ is observed.

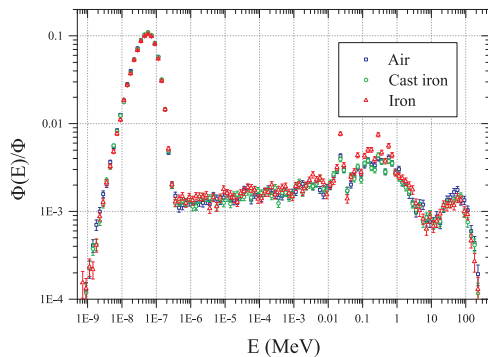


Figure 4: Unitary neutron flux spectra at the beam plane, $\Phi(E)/\Phi$, simulated for three cases of the UCN source inner shielding.

The preliminary results of the activity calculation are given in Fig. 5, and the relative error of $\sim 4\%$ corresponds to the estimated uncertainty of the neutron flux density. The black square in the Fig. 5 shows the preliminary value $1.37 \times 10^6 \pm 15\%$ Bq/g of the measured ^{198}Au specific activity for the gold foil, irradiated at $y = 0.9$ cm above the beam plane. The measured and the calculated value are in good agreement within the error for the case of the cast iron shielding. The calculated difference between the pure and the cast iron cases for the inner shielding is within the simulation error. The comparison of the numerical results for the “air” and cast iron cases shows that the inner shielding is responsible for $\sim 30\%$ increase of the neutron flux around the D_2O tank of the UCN source.

ACKNOWLEDGMENTS

We would like to acknowledge the support of the PSI radiation protection and radioanalysis laboratory personnel with the activity measurements.

ISBN 978-3-95450-122-9

3962

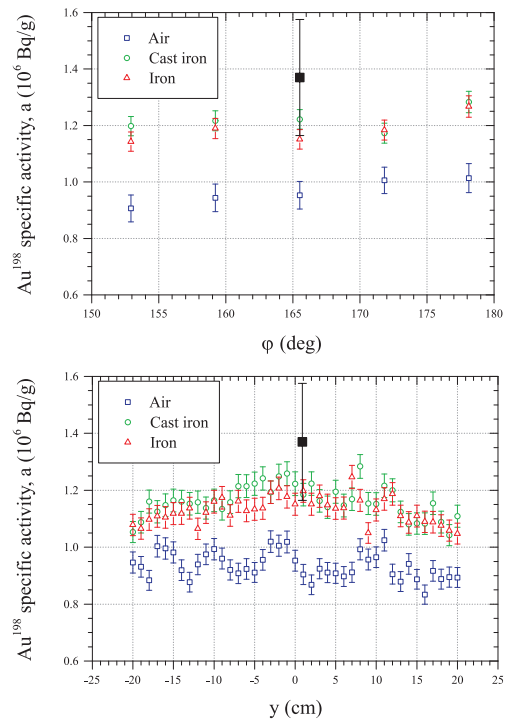


Figure 5: Calculated ^{198}Au specific activity, a (Bq/g), in the gold foil as a function of the azimuthal angle ϕ (top), and as a function of height y (bottom), for three simulated cases of the UCN source inner shielding. The black square shows the preliminary result of the measurement at the beam plane.

REFERENCES

- [1] B. Lauss, “Start-up of the High-intensity Ultracold Neutron Source at the Paul Scherrer Institut,” *Hyp. Int.* 203 (2011) 21.
- [2] Large Research Facilities (GFA) at PSI, <http://gfa.web.psi.ch>
- [3] M. Wohlmuther and G. Heidenreich, “The Spallation Target of the Ultra-cold Neutron Source UCN at PSI,” *Nucl. Instr. and Meth. A* 564 (2006) 51.
- [4] D. Pelowitz (Ed.), “MCNPX User’s Manual. Version 2.7.0,” LA-CP-11-00438, Los Alamos National Laboratory, 2011.
- [5] D. Reggiani, “First Proton Beam Pulses to the UCN Target,” TM-85-10-04, PSI, Villigen, Switzerland (2010).
- [6] F.X. Gallmeier and M. Wohlmuther, “Activation Script Version 1.0 User Guide,” ORNL/TM-2008/031, Oak Ridge National Laboratory (2008).
- [7] F.X. Gallmeier *et al.*, “An Environment Using Nuclear Inventory Codes in Combination with the Radiation Transport Code MCNPX for Accelerator Activation Problems,” In: *Proc. of ACCAPP’07*, Pocatello, Idaho (2007) 207.
- [8] R.A. Forrest, “FISPACT-2003: User manual,” UKAEA FUS 485, EURATOM/UKAEA, Abingdon, UK (2002).
- [9] R.J. McConnell Jr *et al.*, “Compendium of Material Composition Data for Radiation Transport Modelling,” PNNL-15870 Rev. 1, Pacific Northwest National Laboratory (2011).

04 Hadron Accelerators

A14 Neutron Spallation Facilities